Target-selective Protein *S*-Nitrosylation by Sequence Motif Recognition

Jie Jia[1], **Abul Arif**[1], **Fulvia Terenzi**[1], **Belinda Willard**[2], **Edward F. Plow**[3], **Stanley L. Hazen**[1], and **Paul L. Fox**[1,*]

[1]Department of Cellular and Molecular Medicine, The Lerner Research Institute, Cleveland Clinic, Cleveland, OH 44195, USA

[2]Mass Spectrometry Laboratory for Protein Sequencing, The Lerner Research Institute, Cleveland Clinic, Cleveland, OH 44195, USA

[3]Department of Molecular Cardiology, The Lerner Research Institute, Cleveland Clinic, Cleveland, OH 44195, USA

SUMMARY

S-nitrosylation is a ubiquitous protein modification emerging as a principal mechanism of nitric oxide (NO)-mediated signal transduction and cell function. *S*-nitrosylases can use NO synthase (NOS)-derived NO to modify selected cysteines in target proteins. Despite proteomic identification of more than a thousand *S*-nitrosylated proteins, very few *S*-nitrosylases have been identified. Moreover, mechanisms underlying site-selective *S*-nitrosylation and the potential role of specific sequence motifs remain largely unknown. Here, we describe a stimulus-inducible, heterotrimeric *S*-nitrosylase complex consisting of inducible NOS (iNOS), S100A8, and S100A9. S100A9 exhibits transnitrosylase activity, shuttling NO from iNOS to the target protein, whereas S100A8 and S100A9 coordinately direct site selection. A family of proteins *S*-nitrosylated by the iNOS-S100A8/A9 complex were revealed by proteomic analysis, and validated as targets. A conserved I/L-X-C-X$_2$-D/E motif was necessary and sufficient for iNOS- S100A8/A9-mediated *S*-nitrosylation. These results reveal an elusive parallel between protein *S*-nitrosylation and phosphorylation, namely, stimulus-dependent post-translational modification of selected targets by primary sequence motif recognition.

INTRODUCTION

Protein *S*-nitrosylation is a nitric oxide (NO)-dependent post-translational modification of cysteine that regulates protein structure and function in bacteria, plants, and mammals (Nakamura et al., 2013; Seth et al., 2012; Yun et al., 2011). An activated NO moiety is

*Correspondence: foxp@ccf.org.

covalently added to the free thiol group on cysteine, generating an *S*-nitrosothiol. High-throughput proteomic approaches have identified more than a thousand *S*-nitrosylated (SNO –) proteins and linked to diverse cellular functions (Doulias et al., 2010; Seth and Stamler, 2011). Physiological *S*-nitrosylation contributes to cellular homeostasis, whereas, dysregulation can lead to severe pathological consequences (Haldar and Stamler, 2013; Lim et al., 2008a; Nakamura et al., 2013).

Like phosphorylation and ubiquitination, protein *S*-nitrosylation is regulatable, reversible, and target- and site-selective. However, the mechanism underlying selectivity has remained elusive. The eukaryotic nitric oxide synthase (NOS) family has three cell-selective isoforms, neuronal NOS (nNOS), inducible NOS (iNOS), and endothelial NOS (eNOS). There is limited evidence that NOS can mediate selective *S*-nitrosylation via direct NOS-substrate interactions (Fang et al., 2000; Garcia-Cardena et al., 1998; Kim et al., 2005); however, this mechanism is unlikely to account for selective targeting of Cys residues in a multitude of distinct protein substrates by only three NOS isoforms. An alternative adaptor mechanism is supported by reports that certain SNO-proteins have *S*-nitrosylase activity and can transfer NO from its own S-nitrosothiol group to a free thiol on a target protein via direct protein-protein interaction. Fewer than ten *S*-nitrosylases have been identified to date (Nakamura and Lipton, 2013), and the primary sequences and structures that establish the rules governing specificity of substrate recognition and cysteine transnitrosylation are largely unknown. Recent global analyses of *S*-nitrosocysteine sites revealed information on specific determinants of S-nitrosylation, but failed to identify a primary sequence motif for site-selective S-nitrosylation (Doulias et al., 2010; Hao et al., 2006; Marino and Gladyshev, 2010). Together, these findings suggest that additional *S*-nitrosylases, mechanisms, and motifs are yet to be revealed.

Glyceraldehyde 3-phosphate dehydrogenase (GAPDH) is a key glycolytic enzyme and a well-studied *S*-nitrosylation target. *S*-nitrosylation of GAPDH regulates enzymatic activity (Padgett and Whorton, 1995), but also mediates several "moonlighting" functions (Jia et al., 2012; Kornberg et al., 2010). Recently, we reported that selective, inducible *S*-nitrosylation of GAPDH dysregulates translational control of gene expression by the interferon-gamma (IFN-γ)-activated inhibitor of translation (GAIT) complex (Jia et al., 2012). GAPDH, along with ribosomal protein L13a, Glu-Pro tRNA synthetase (EPRS), and NS1-associated protein are induced by IFN-γ to form the GAIT complex (Sampath et al., 2004) that inhibits translation of vascular endothelial growth factor-A (*VEGF-A*) and other inflammation-related mRNAs (Ray et al., 2009; Vyas et al., 2009). Low-density lipoprotein (LDL) that is oxidatively-modified (LDL_{ox}) by the physiological myeloperoxidase (MPO) system suppresses GAIT system activity by selective S-nitrosylation of GAPDH Cys[247], a residue distant from the catalytic domain. *S*-nitrosylated GAPDH fails to bind and protect L13a, leading to ubiquitination and proteasomal degradation of L13a, and consequent GAIT system inactivation. Here we elucidate the molecular mechanism underlying stimulus-dependent, site-selective *S*-nitrosylation of GAPDH, revealing an inducible heterotrimeric *S*-nitrosylase complex, and a consensus motif that directs specific S-nitrosylation on multiple target proteins.

RESULTS

iNOS Is Required For LDL$_{ox}$/IFN-γ-Inducible *S*-nitrosylation of GAPDH Cys[247]

To determine the role of enzymatically generated NO in GAPDH *S*-nitrosylation, NOS inhibitors were used. Human peripheral blood monocytes (PBM) were transfected with HA-tagged GAPDH (HA-GAPDH) plasmids bearing Cys-to-Ser mutations at each of the 3 Cys residues, or wild-type. Cells were then incubated with IFN-γ and LDL$_{ox}$ for 24 hr in the presence of the non-selective NOS inhibitor, L-NMMA (NG-monomethyl-L-arginine acetate). The biotin-switch assay revealed specific *S*-nitrosylation of GAPDH at Cys[247], and suppression by L-NMMA (Figure 1A). Also, GAPDH *S*-nitrosylation was completely suppressed by 1400W (Figure 1B), which exhibits a 1000-fold selectivity for iNOS, the principal myeloid cell isoform (Garvey et al., 1997; Hara et al., 2005). IFN-γ and LDL$_{ox}$ markedly induced iNOS mRNA and protein in PBM; however, the individual agonists were only modestly stimulatory (Figure 1C). iNOS-specific siRNA blocked iNOS induction and GAPDH *S*-nitrosylation supporting its critical role (Figure 1D).

LDL$_{ox}$/IFN-γ Induces iNOS and Its Interaction with GAPDH

In addition to functioning as the major NO source, NOS isoforms can direct selective *S*-nitrosylation by interaction with targets. LDL$_{ox}$/IFN-γ, but not with LDL/IFN-γ or IFN-γ alone, induced the binding of iNOS to GAPDH (Figure 1E). To determine the specific role of LDL$_{ox}$ in the iNOS-GAPDH interaction, U937 cells were transfected with His-tagged iNOS and then treated with LDL$_{ox}$ for 24 hr in absence of IFN-γ. LDL$_{ox}$ by itself was sufficient to induce protein interaction, thus revealing a dual function of LDL$_{ox}$ in both iNOS induction and interaction with GAPDH (Figure 1F). To determine whether iNOS by itself is sufficient for GAPDH *S*-nitrosylation, cells were transfected with His-iNOS but *S*-nitrosylation was not observed in the absence of LDL$_{ox}$/IFN-γ, indicating iNOS is necessary but not sufficient for modification (Figure 1G).

Dysregulation of GAIT System by LDL$_{ox}$/IFN-γ Requires iNOS

To establish the role of iNOS in GAPDH S-nitrosylation and L13a degradation, bone marrow-derived macrophages (BMDM) isolated from iNOS$^{-/-}$ and wild-type mice were incubated with IFN-γ or LDL$_{ox}$ or both. LDL$_{ox}$/IFN-γ-inducible *S*-nitrosylation of GAPDH was observed in BMDM from wild-type but not iNOS$^{-/-}$ mice (Figure 1H). Likewise, GAPDH-L13a interaction was not inhibited by LDL$_{ox}$/IFN-γ in iNOS$^{-/-}$ BMDM, subsequently preventing L13a degradation. Finally, we investigated the role of iNOS$^{-/-}$ in GAIT system inactivation by LDL$_{ox}$/IFN-γ that prevents delayed translational silencing of GAIT element-bearing target mRNAs, e.g., VEGF-A and ceruloplasmin (Cp), thereby prolonging their expression (Jia et al., 2012). Synthesis of VEGF-A and Cp in agonist-treated BMDM was determined by ^{35}S-Met metabolic labeling. BMDM from wild-type mice exhibited translational silencing after 24 hr of IFN-γ treatment that was prevented by LDL$_{ox}$ (Figure 1I). Likewise, expression of GAIT targets was silenced by IFN-γ in BMDM from iNOS$-/-$ mice. However, LDL$_{ox}$ failed to prevent the inhibition, consistent with a critical role of iNOS-driven *S*-nitrosylation of GAPDH in regulating GAIT system activity.

S100A8/9 Complex Mediates Binding of iNOS to GAPDH

Human GAPDH is a multifunctional protein containing Cys residues at 152, 156, and 247. LPS-stimulated *S*-nitrosylation of GAPDH Cys[152] contributes to its role in apoptotic signaling and heme trafficking (Chakravarti et al., 2010; Hara et al., 2005), whereas LDL$_{ox}$/IFN-γ-stimulated *S*-nitrosylation of Cys[247] prevents GAIT system activation (Jia et al., 2012). Like Cys[247] *S*-nitrosylation, iNOS is essential for Cys[152] S-nitrosylation as well (Hara et al., 2005). However, in neither case is the mechanism of selective *S*-nitrosylation known. Differential nitrosylation of distinct sites by iNOS suggests potential recruitment of other proteins to provide site selectivity. To identify interacting proteins, lysates from LDL$_{ox}$/IFN-γ-treated PBM were immunoprecipitated with anti-iNOS or anti-GAPDH antibody, and resolved by electrophoresis and silver stain (Figure 2A). Proteins in enriched bands were identified by liquid chromatography-tandem mass spectrometry (LC-MS) (Table S1). Two proteins, histone H2A and S100A9, were captured by both antibodies. However, immunoblot analysis failed to show an interaction between H2A and iNOS or GAPDH (Figure S1). S100A9 is an inflammatory mediator that forms a heterodimeric complex with S100A8 in myeloid cells (Roth et al., 2003). Notably, S100A8 was also detected by LC-MS (Table S1). Detection of iNOS and GAPDH, as positive controls, validated the approach. LDL$_{ox}$/IFN-γ did not induce expression of S100A8 or S100A9 (Figure 2B), but led to the inducible assembly of a complex containing all four proteins (Figure 2C). In the absence of stimulation, only S100A8 and S100A9 were found to interact.

We used a knockdown approach to determine whether S100A8 and S100A9 are necessary for interaction of the NO donor, iNOS, with its target, GAPDH. Depletion of GAPDH did not disrupt iNOS binding to S100A8/A9, and S100A8 depletion did not block the interaction of the other three components (Figure 2D, left). However, S100A9 depletion prevented the binding of iNOS to GAPDH and S100A8, suggesting S100A9 is an indispensable intermediary for iNOS interaction with its *S*-nitrosylation target, GAPDH (Figure 2D, right). To determine the specific stimulus-dependence of iNOS binding to S100A8/A9, PBM were transfected with His-iNOS. LDL$_{ox}$ by itself, but not IFN-γ, was sufficient to induce the interaction of iNOS with S100A8/A9 (Figure 2E). Because LDL$_{ox}$ induces Ca^{2+} flux in leukocytes (van Tits et al., 2000) and both S100A8 and S100A9 are Ca^{2+}-binding proteins (Hessian et al., 1993), we investigated the role of Ca^{2+} in complex assembly. In PBM ectopically expressing His-iNOS, LDL$_{ox}$ induced a 2.9-fold increase in cytosolic Ca^{2+}, iNOS binding to S100A8/A9, and GAPDH *S*-nitrosylation (Figure 2F). Ca^{2+} chelators BAPTA-AM or EGTA suppressed Ca^{2+} induction by LDL$_{ox}$, and inhibited iNOS-S100A8/A9 complex assembly and GAPDH *S*-nitrosylation. Ca^{2+} ionophores A23187 and ionomycin raised intracellular Ca^{2+} to levels comparable to LDL$_{ox}$-treated cells, but did not induce complex assembly, suggesting Ca^{2+} is necessary but not sufficient for LDL$_{ox}$-induced *S*-nitrosylation.

Transnitrosylase Activity of S100A9 is Essential for GAPDH Cys[247] *S*-Nitrosylation

S100A9 knockdown prevented inducible GAPDH *S*-nitrosylation, whereas S100A8 knockdown was ineffective, indicating S100A9 is essential for GAPDH *S*-nitrosylation (Figure 3A). We investigated the hypothesis that S100A9 not only mediates iNOS-GAPDH interaction, but also acts as a functional couple, transferring iNOS-derived NO to its target.

LDL_{ox}/IFN-γ induced iNOS-dependent S-nitrosylation of S100A9 in PBM (Figure 3B). We considered the possibility that SNO-S100A9 acts as an *S*-nitrosylase, transferring the NO moiety to GAPDH. Purified S100A9 protein was subjected to *in vitro S*-nitrosylation by GSNO or GSH as negative control. After desalt, GSNO-modified S100A9 was incubated with purified GAPDH protein. GSNO led to S-nitrosylation of S100A9 that in turn induced GAPDH S-nitrosylation (Figure 3C). We determined the requirement for Cys[3], the sole cysteine in human S100A9, for transnitrosylase activity. Endogenous S100A9 expression in PBM was silenced by 3′UTR-specific siRNA, and replenished by co-transfection with myc-S100A9, wild-type or C3A mutant. S100A9 *S*-nitrosylation was abolished by S100A9 knockdown, as was GAPDH S-nitrosylation. Recombinant wild-type S100A9, but not C3A mutant, restored GAPDH S-nitrosylation, verifying the critical role of Cys[3] (Figure 3D). In addition, S100A9 knockdown rescued L13a from inducible degradation, and restored GAIT-directed suppression of VEGF-A, establishing the link between S100A9 and translational control by the GAIT system. LDL_{ox}/IFN-γ induced *S*-nitrosylation of wild-type S100A9 and binding to both iNOS and S100A8 (Figure 3E). The C3A mutant interacted with S100A8 but failed to bind iNOS, suggesting Cys[3] *S*-nitrosylation is required for complex assembly, consistent with an important role of S-nitrosylation in protein interaction as described previously (Hess et al., 2005; Marozkina and Gaston, 2012).

S100A8 Contributes to Site-selectivity of *S*-Nitrosylase Complex in GAPDH S-Nitrosylation

In contrast to S100A9, S100A8 depletion did not disrupt the iNOS-GAPDH interaction or prevent GAPDH *S*-nitrosylation (Figure 2D, 3A). We considered the possibility that S100A8 contributes to target specificity of *S*-nitrosylation. PBM were co-transfected with S100A8 siRNA and HA-GAPDH. Control cells treated with scrambled siRNA exhibited specific stimulus-inducible *S*-nitrosylation of GAPDH Cys[247] as shown by the total absence of modification of the C247S mutant (Figure 4A). Remarkably, S100A8 knockdown permitted *S*-nitrosylation of C247S mutant indicating a loss of target specificity, and suggesting S100A8 directs site selectivity of the iNOS-S100A8/A9 *S*-nitrosylase complex. S100A8 depletion permitted *S*-nitrosylation of GAPDH Cys[247] and Cys[152], but not Cys[156] (Figure 4B).

To elucidate the mechanism of S100A8-directed site-selection, the interaction of S100A8 and GAPDH was probed by His-tag pull-down. Purified GAPDH specifically bound recombinant human S100A8, but not EPRS WHEP-R1 control protein (Jia et al., 2008) (Figure 4C). The GAPDH region that interacts with S100A8 was probed using the FeBABE (Fe(III) (s)-1-(*p*-bromoacetamidobenzyl) EDTA) "artificial protease" method. The sole cysteine in S100A8, Cys[42], was mutated to serine, and cysteine residues were introduced into S100A8 at 10-amino acid intervals for covalent labeling with FeBABE. The site of interaction between HA-GAPDH and FeBABE-labeled S100A8 was detected by FeBABE-directed, hydroxyl radical-mediated cleavage mapping. Wild-type S100A8 and three mutants (I22C/C42S, D32C/C42S, and D52C/C42S) caused marked cleavage of GAPDH in helices α1 and α3 (Figure 4D). Importantly, GAPDH Cys[247] is located near the termini of both helices, suggesting S100A8 may contribute to specific GAPDH *S*-nitrosylation by proximity to the target cysteine (Figure 4E), possibly by altering the nearby structure. We applied Förster resonance energy transfer (FRET) to probe the S100A8-inducible

conformational shift. GAPDH Cys[156] was mutated to Ser to generate a FRET donor-acceptor pair of Cys[152] and Cys[247] for dye labeling. GAPDH C156S was labeled with mixed thiol-reactive dyes, Alexa 546- and 647-C5-maleimide. The apparent mean interfluor distance for GAPDH by itself was calculated to be 51.6 Å and increased to 58.0 Å by addition of S100A8 (Figure S2), indicative of a substantial conformational shift, consistent with *S*-nitrosylation of tetrameric GAPDH as the X-ray structure (Ismail and Park, 2005) indicates the distance between the Cys-Cys pair in the monomer is 21 Å, whereas the maximum distance in the tetramer is 64.8 Å (Ismail and Park, 2005).

iNOS-S100A8/A9 Directs Selective *S*-nitrosylation of Multiple Targets

We applied a global, proteomic approach to assess whether iNOS-S100A8/A9 nitrosylates other proteins. S100A9-depleted or untreated human PBM were incubated with LDL$_{ox}$/IFN-γ for 24 hr, and *S*-nitrosylated proteins in lysates were subjected to biotin-switch labeling and streptavidin-agarose pulldown. Following electrophoresis and Coomassie blue stain, bands identified in untreated, but not in S100A9-depleted cells, were selected for LC-MS analysis, and an ensemble of 95 SNO-protein candidates, including GAPDH and S100A9, were identified (Table S2).

LDL$_{ox}$/IFN-γ-inducible S-nitrosylation was determined for candidates having only 1 or 2 cysteines, thereby facilitating detailed analysis. Five of the nine candidates, annexin V, ezrin, HSPA5, moesin, and vimentin, exhibited robust, stimulus-inducible *S*-nitrosyla-tion (Figure 5A, left). 1400W inhibited *S*-nitrosylation of all five candidates, indicating the requirement for iNOS. Four candidates were not *S*-nitrosylated indicating either false-positive LC-MS results, or possibly co-precipitation with *S*-nitrosylated interacting partners (Figure 5A, right). S100A9-depletion suppressed *S*-nitrosylation of annexin V, ezrin, moesin, and vimentin (Figure 5B). Unexpectedly, HSPA5 *S*-nitrosylation was not affected by S100A9 depletion indicative of modification by an S100A9-independent *S*-nitrosylase.

The possibility that a specific motif directs modification by iNOS-S100A8/A9 was explored by sequence alignment. 21 amino acids surrounding all 7 cysteine residues in five validated target SNO-proteins (ezrin and moesin each contain two cysteines) were aligned. A conserved I/L-X-C-X$_2$-D/E sequence is present at Cys[247] in GAPDH, in the two validated SNO-proteins containing a single cysteine, and in one of two cysteines in the other two validated proteins, but not in the non-validated proteins or at Cys[152] or Cys[156] in GAPDH (Figures 5C).

S-Nitrosylation Motif Directs Selective Target Recognition by iNOS-S100A8/A9

The function of the putative sequence motif was tested in GAPDH. Cys[152] and Cys[156] were mutated to Ser to restrict analysis to Cys[247]. Site-directed mutagenesis of Leu[245] or Glu[250], or both, in the consensus motif markedly abrogated LDL$_{ox}$/IFN-γ-inducible *S*-nitrosylation of GAPDH at Cys[247] (Figure 6A, top). GSNO induced *S*-nitrosylation of wild-type and all mutant GAPDH isoforms equally showing a complete absence of target-specific *S*-nitrosylation by GSNO (Figure 6A, bottom). To characterize the role of S100A8 in motif recognition, *S*-nitrosylation of motif mutants was assessed in S100A8-deficient cells. Unexpectedly, S100A8 depletion restored inducible *S*-nitrosylation of Cys[247] in the Leu[245]

mutant, but not in the Glu^{250} or double mutant, suggesting Leu^{245} is necessary for motif recognition by S100A8 and Glu^{250} is recognized by iNOS/S100A9 (Figure 6B). The GAPDH crystal structure indicates surface-accessibility of the three motif residues (Figure 6C).

To explore motif universality, the SNO-site of human moesin was investigated. Cys^{117} and Cys^{284} were individually mutated to Ser. LDL$_{ox}$/IFN-γ was unable to induce *S*-nitrosylation of C117S moesin indicating Cys^{117} is the sole *S*-nitrosylation site (Figure 6D; E, left). In contrast to the loss of target specificity observed for GAPDH, depletion of S100A8 did not alter *S*-nitrosylation site selection in moesin, suggesting a possible steric constraint prevents transfer of the NO moiety (Figure 6E, left; F). Cys^{117} is within a predicted S-nitrosylation motif with Ile^{115} and Glu^{120}. As expected, LDL$_{ox}$/IFN-γ induced S-nitrosylation of wild-type moesin and the C284S mutant, but not motif-negative mutants containing I115M or E120M, or both (Figure 6E, right; G). S100A8 depletion restored S-nitrosylation of Ile^{115} mutant, however, the Glu^{120} mutation still blocked S-nitrosylation of moesin (Figure 6H). Consistent with GAPDH motif recognition, this result suggests a general rule in which the I/L residue is recognized by S100A8 and D/E is critical for S-nitrosylation by iNOS/S100A9 (Figure 7A). Together these experiments show that both the upstream and downstream components of the I/L-X-C-X$_2$-D/E motif are required for LDL$_{ox}$/IFN-γ induced S-nitrosylation.

To determine whether the motif is sufficient for *S*-nitrosylation, a gain-of-function approach was explored using moesin as target. We observed that the Cys^{117}-containing motif is surface accessible and near the terminus of an α-helix. As a target we selected a nearby surface accessible site near the terminus of a nearby α-helix (H^{161}-X-L^{163}-X$_2$-D^{166}) (Figure 6E, right). To eliminate background *S*-nitrosylation, Cys^{117} and Cys^{284} were mutated to serine. The endogenous H^{161}-X-L^{163}-X$_2$-D^{166} sequence was mutated stepwise to generate I^{161}-X-C^{163}-X$_2$-E^{166}, which conforms to the consensus *S*-nitrosylation motif. Moesin with a Cys residue inserted by an L163C mutation failed to be *S*-nitrosylated by LDL$_{ox}$/IFN-γ treatment (Figure 6I). However, the H161I/L163C double mutant was efficiently *S*-nitrosylated. Likewise, a H161I/L163C/D166E triple mutant was modified revealing a similar effectiveness of Asp and Glu.

DISCUSSION

S-nitrosylation has emerged as a dominant regulatory mechanism in NO-associated signal transduction and cell function (Gould et al., 2013; Smith and Marletta, 2012). More than 3,000 *S*-nitrosocysteine sites have been identified by proteomic analysis of *in vitro* and *in vivo S*-nitrosylated proteins (Chen et al., 2010). Despite the extreme diversity, the apparent fidelity and site-selective nature of the modification suggests precise regulation of the *S*-nitrosylation process (Seth and Stamler, 2011). Using biochemical and genetic approaches, we have identified a stimulus-activated *S*-nitrosylase complex that directs motif-dependent protein S-nitrosylation in human myeloid cells (Figure 7). IFN-γ and LDL$_{ox}$ synergistically induce iNOS expression, and initiate the assembly of a *S*-nitrosylase complex consisting of iNOS and S100A8/A9. LDL$_{ox}$-inducible interaction of iNOS to S100A8 and S100A9, both calcium-binding proteins, is accompanied by induction of intracellular Ca^{2+}, which may be

mediated by the CD36 receptor and the Lyn/Fyn-Vav signaling pathway (Rahaman et al., 2011). Although S100A8 *S*-nitrosylated *in vitro* by GSNO can slowly transfer the NO group to hemoglobin (Lim et al., 2008b), the function of intracellualr S100A8/A9 in S-nitrosylation has not been investigated. In our studies, we show that S100A9 acts both as an adaptor linking iNOS to its target via protein-protein interaction, and as a transnitrosylase that transfers the NO moiety from iNOS to its target, via its own *S*-nitrosylated Cys[3]. S100A8 interacts with the target and dictates site-specificity of the *S*-nitrosylase complex by motif recognition. S100A8 binding induces a conformational change in the target protein and restricts transfer of NO from S100A9 to the motif-associated cysteine.

All three NOS isoforms act as NO donors for target-selective *S*-nitrosylation *in vivo* (Seth and Stamler, 2011). Importantly, individual NOS isoforms can direct selective *S*-nitrosylation of distinct cysteine residues in the same protein. In one well-studied example, iNOS induces GAPDH *S*-nitrosylation at either Cys[152] (Hara et al., 2005) or Cys[247] (Figure 1) in distinct cell types and in response to distinct stimuli, most clearly illustrating both high-level specificity as well as the utilization of multiple mechanisms. The recognition of a multitude of targets by just three NOS isoforms distinguishes *S*-nitrosylation from phosphorylation, a site-specific post-translational modification mediated by about 950 human kinases (Buzko and Shokat, 2002). Multiple adaptor proteins might contribute to the specificity problem of substrate recognition by NOS isoforms. Supporting this mechanism, PSD-95 (Lipton et al., 2002) and CAPON (Fang et al., 2000) act as scaffolds that direct nNOS binding to its *S*-nitrosylation targets. This mechanism is analogous to the polyubiquitination system in which one of about 520 E3 ubiquitin ligases act as adaptors to direct binding of the catalytic E2 ubiquitin-conjugating enzymes that transfer ubiquitin to the target lysine residue (Li et al., 2008). The adaptor mechanism in site-selective *S*-nitrosylation is supported by our finding that S100A8/A9 directs the binding of iNOS to GAPDH. However, S100A8/A9 also exhibits transnitrosylase activity, transferring the NO group from the iNOS donor to GAPDH, as well as to four other validated targets and about 90 other candidates. Interestingly, nNOS *S*-nitrosylates PSD-95 at Cys[3] and Cys[5] (Ho et al., 2011), but their role in NMDAR *S*-nitrosylation, and the possible function of PSD-95 as an nNOS-associated *S*-nitrosylase, has not been determined.

Despite considerable effort, a specific consensus sequence or motif that directs *S*-nitrosylation globally or in an ensemble of proteins has not been identified (Doulias et al., 2010; Marino and Gladyshev, 2010; Seth and Stamler, 2011). The difficulty of deconvolving the signal of a dominant motif from a multitude of sequences targeted by diverse *S*-nitrosylases and adaptors has rendered this problem nearly insoluble. The complexity of the problem is multiplied further by the diminished specificity of *S*-nitrosylation by chemical NO donors that that can generate up to 1000 SNO-proteins. We took advantage of an analysis of a select family of SNO-proteins, revealed by proteomic analysis and experimentally validated to be specifically *S*-nitrosylated by the iNOS-S100A8/A9 complex. A consensus I/L-X-C-X$_2$-D/E motif was observed in five *S*-nitrosylated proteins. Disruption of conserved residues I/L and/or D/E in the motif blocked S-nitrosylation in both proteins tested at the predicted sites, Cys[247] of GAPDH and Cys[117] of moesin. Mutation of amino acids in the consensus motif did not inhibit *S*-nitrosylation of GAPDH Cys[247] by GSNO,

consistent with previous reports of lack of specificity of GAPDH *S*-nitrosylation by GSNO (Paige et al., 2008; Wu et al., 2011). Exogenous, non-enzymatic donors induce high, non-physiological intracellular NO concentrations, that can direct non-selective *S*-nitrosylation of free, surface-accessible cysteine residues. The dissimilar, site-specific *S*-nitrosylation of GAPDH at Cys[152] by apoptotic agonists suggests the activity of a distinct *S*-nitrosylase and cognate motif (Hara et al., 2005). Certainly, the I/L-X-C-X_2-D/E motif is not required for all, or even most site-selective protein nitrosylations, as exemplified by apoptosis-driven stimulation of *S*-nitrosylation of GAPDH Cys[152], which is not located within the consensus motif. More interestingly, HSPA5 is subject to LDL$_{ox}$/IFN-γ-stimulated *S*-nitrosylation but neither of the two cysteine residues are contained within the consensus motif, and the modification requires iNOS, but not S100A8/A9. This result indicates that a single stimulatory condition, i.e., LDL$_{ox}$/IFN-γ, can activate site-selective *S*-nitrosylation by multiple mechanisms.

Several structural factors have been suggested to contribute to protein *S*-nitrosylation, including acid-base sequences in residues within 6–8 angstroms (Marino and Gladyshev, 2010), nearby hydrophobic residues (Seth and Stamler, 2011), high nucleophilicity (Hess et al., 2005), helical structure, and solvent accessibility (Doulias et al., 2010). Interestingly, the I/L-X-C-X_2-D/E motif described here exhibits most, if not all, of these characteristics. The Cys residue is surrounded by a nearby acidic residue, D/E, and a hydrophobic residue, I/L, which can increase cysteine nucleophilicity. In addition, according to X-ray crystal structures, the *S*-nitrosylated cysteine in each of the validated SNO-proteins is solvent-accessible, and located within or adjacent to α-helical domains (Edwards and Keep, 2001; Huber et al., 1992; Nicolet et al., 2010; Smith et al., 2003). The I/L-X-C-X_2-D/E motif is present in 19 additional candidate SNO-proteins revealed by our proteomic analysis (Table S2), suggesting a wide-ranging role in *S*-nitrosylation. Ontologic analysis of motif-bearing candidates suggests linkage to cytoskeleton organization, cell movement, catabolic processes, inflammation, and protein localization (Huang da et al., 2009). Analysis of a SNO-protein database that includes 810 SNO-peptides in 445 human proteins (Lee et al., 2012) revealed only 15 peptides in 15 proteins contain the I/L-X-C-X_2-D/E motif. This result is consistent with a relatively high specificity and low occurrence of nitrosylation by the iNOS-S100A8/A9 complex compared to chemical NO donors. S100A9, in the absence of S100A8, has the potential to increase the target range by recognition of a less stringent CX_2D/E motif (Figure 6B, 6H). However, this situation may not be physiologically relevant because S100A9 by itself is unstable (Riva et al., 2013). Likewise, rapid turnover of S100A8 in S100A9-null mice suggests heterodimer formation is important to maintain expression and function of the complex (Hobbs et al., 2003).

S100A8 and S100A9 are constitutively expressed in myeloid cells and predominantly found as a heterodimeric complex *in vivo*. S100A8/A9 comprises about 1% of total protein in monocytes attesting to its potential pathophysiological significance (Edgeworth et al., 1991). S100A8/A9 is generally considered to be a pro-inflammatory agent, however, the specific cellular functions of S100A8/A9 are incompletely understood (Goyette and Geczy, 2011; Roth et al., 2003). Release of S100A8/A9 by activated neutrophils, monocytes, and platelets has led to a primary focus on the extracellular functions. Its plasma level in humans is

associated with increased risk for CVD (Ma et al., 2012; Nagareddy et al., 2013), possibly by contributing to both innate and adaptive immune responses. The complex is particularly abundant in inflammatory sites, including atherosclerotic lesions of mice and humans, and its level correlates with characteristics or rupture-prone plaques (Croce et al., 2009; Ionita et al., 2009; McCormick et al., 2005). Genetic deletion of S100A9 decreases atherosclerotic lesion formation in apoE$^{-/-}$ mice (Croce et al., 2009). Possibly, S100A9 depletion restores GAIT system activity by blocking GAPDH Cys^{247} S-nitrosylation and L13a degradation thereby suppressing expression of inflammation-related proteins. However, the stimulatory role of S100A8/A9 in atherosclerotic lesion formation has not been uniformly observed in other mouse models (Averill et al., 2011; Croce et al., 2009). Interestingly, both S100A9 and iNOS are enriched in macrophage-rich regions in the Alzheimer's disease (AD) brain, and depletion of either provides significant clinical benefits in animal models of AD (Ha et al., 2010; Nathan et al., 2005). Recent studies of differential protein *S*-nitrosylation revealed 45 AD-associated SNO-proteins in humans and 33 in mouse models of AD (Zahid et al., 2014; Zareba-Koziol et al., 2014). Interestingly, 6 human and 6 mouse AD-associated SNO-proteins contain the I/L-X-C-X$_2$-D/E motif.

The intracellular activities of S100A8/A9, and particularly their potential contributions to cellular inflammation remain largely unexplored. S100A8/A9 may contribute to myeloid cell inflammation via S-nitrosylation of inflammatory mediators in addition to GAPDH. Several candidate or validated SNO-proteins revealed by our analysis are linked to myeloid cell inflammatory processes, such as CAP1 (Lee et al., 2014), SAMHD1 (Laguette et al., 2011). Moreover, S100A8/A9 has been implicated in additional intracellular functions, including cytoskeleton organization (Vogl et al., 2004) and gene regulation (Schonthaler et al., 2013). Our discovery of an inflammatory stimulus-dependent *S*-nitrosylase complex, and its recognition motif, opens a new avenue of thought in deciphering the role of *S*-nitrosylation in inflammation, the specific participants, and the underlying molecular mechanisms.

EXPERIMENTAL PROCEDURES

For additional details, see Extended Experimental Procedures.

Biotin-Switch and Protein *S*-Nitrosylation Assay

Cell lysates (1 mg protein) were subjected to biotin-switch labeling as described (Jia et al., 2012) by using *S*-nitrosylated Protein Detection Kit (Cayman). *In vitro* transnitrosylase activity of S100A9 was determined as described (Kornberg et al., 2010). Purified S100A9 protein was incubated with 100 μM GSH control or GSNO in the dark for 30 min at room temperature. After desalting, S100A9 was incubated with purified GAPDH for additional 30 min, and then subjected to biotin-switch analysis.

S100A8-GAPDH Interaction Experiments

S100A8-GAPDH interaction was determined *in vitro* using His Protein Interaction Pull-down Kit (Pierce). His-S100A8 and His- WHEP-R1 were expressed in E.coli and purified. 1 nmol His-protein was immobilized on cobalt agarose resin, and then incubated with 2-fold

molar excess of purified GAPDH for 1 hr. Eluted protein was subjected to electrophoresis and immunoblot analysis.

The FeBABE (Fe(III) (s)-1-(*p*-bromoacetamidobenzyl) EDTA) "artificial protease" method was used for mapping S100A8 interacting sites on GAPDH. The sole cysteine in S100A8, Cys[42], was mutated to serine, and additional cysteine was introduced into S100A8 at 10-amino acid intervals for covalent labeling with FeBABE, and the proteins expressed in *E. coli* and purified. 10 nmol S100A8 was labeled using FeBABE Protein Interaction Mapping Kit (Pierce) according to manufacture's protocol. 50 pmol HA-GAPDH was mixed with equimolar FeBABE-labeled S100A8 for 1 hr, and subjected to FeBABE-directed, hydroxyl radical-mediated cleavage mapping. Samples were immediately subjected to electrophoresis and IB with anti-HA tag antibody. Cleavage sites were determined within 8–10 residues by determining the molecular weight of GAPDH fragments based on standard protein markers as described (Chen and Hahn, 2003).

Supplementary Material

Refer to Web version on PubMed Central for supplementary material.

Acknowledgments

References

Averill MM, Barnhart S, Becker L, Li X, Heinecke JW, Leboeuf RC, Hamerman JA, Sorg C, Kerkhoff C, Bornfeldt KE. S100A9 differentially modifies phenotypic states of neutrophils, macrophages, and dendritic cells: implications for atherosclerosis and adipose tissue inflammation. Circulation. 2011; 123:1216–1226. [PubMed: 21382888]

Buzko O, Shokat KM. A kinase sequence database: sequence alignments and family assignment. Bioinformatics. 2002; 18:1274–1275. [PubMed: 12217924]

Chakravarti R, Aulak KS, Fox PL, Stuehr DJ. GAPDH regulates cellular heme insertion into inducible nitric oxide synthase. Proc Natl Acad Sci U S A. 2010; 107:18004–18009. [PubMed: 20921417]

Chen HT, Hahn S. Binding of TFIIB to RNA polymerase II: Mapping the binding site for the TFIIB zinc ribbon domain within the preinitiation complex. Mol Cell. 2003; 12:437–447. [PubMed: 14536083]

Chen YJ, Ku WC, Lin PY, Chou HC, Khoo KH. S-alkylating labeling strategy for site-specific identification of the s-nitrosoproteome. J Proteome Res. 2010; 9:6417–6439. [PubMed: 20925432]

Croce K, Gao H, Wang Y, Mooroka T, Sakuma M, Shi C, Sukhova GK, Packard RR, Hogg N, Libby P, et al. Myeloid-related protein-8/14 is critical for the biological response to vascular injury. Circulation. 2009; 120:427–436. [PubMed: 19620505]

Doulias PT, Greene JL, Greco TM, Tenopoulou M, Seeholzer SH, Dunbrack RL, Ischiropoulos H. Structural profiling of endogenous S-nitrosocysteine residues reveals unique features that accommodate diverse mechanisms for protein S-nitrosylation. Proc Natl Acad Sci U S A. 2010; 107:16958–16963. [PubMed: 20837516]

Edgeworth J, Gorman M, Bennett R, Freemont P, Hogg N. Identification of p8, 14 as a highly abundant heterodimeric calcium binding protein complex of myeloid cells. J Biol Chem. 1991; 266:7706–7713. [PubMed: 2019594]

Edwards SD, Keep NH. The 2.7 A crystal structure of the activated FERM domain of moesin: an analysis of structural changes on activation. Biochemistry. 2001; 40:7061–7068. [PubMed: 11401550]

Fang M, Jaffrey SR, Sawa A, Ye K, Luo X, Snyder SH. Dexras1: a G protein specifically coupled to neuronal nitric oxide synthase via CAPON. Neuron. 2000; 28:183–193. [PubMed: 11086993]

Garcia-Cardena G, Fan R, Shah V, Sorrentino R, Cirino G, Papapetropoulos A, Sessa WC. Dynamic activation of endothelial nitric oxide synthase by Hsp90. Nature. 1998; 392:821–824. [PubMed: 9580552]

Garvey EP, Oplinger JA, Furfine ES, Kiff RJ, Laszlo F, Whittle BJ, Knowles RG. 1400W is a slow, tight binding, and highly selective inhibitor of inducible nitric-oxide synthase in vitro and in vivo. J Biol Chem. 1997; 272:4959–4963. [PubMed: 9030556]

Gould N, Doulias PT, Tenopoulou M, Raju K, Ischiropoulos H. Regulation of protein function and signaling by reversible cysteine S-nitrosylation. J Biol Chem. 2013; 288:26473–26479. [PubMed: 23861393]

Goyette J, Geczy CL. Inflammation-associated S100 proteins: new mechanisms that regulate function. Amino Acids. 2011; 41:821–842. [PubMed: 20213444]

Ha TY, Chang KA, Kim J, Kim HS, Kim S, Chong YH, Suh YH. S100a9 knockdown decreases the memory impairment and the neuropathology in Tg2576 mice, AD animal model. PLoS One. 2010; 5:e8840. [PubMed: 20098622]

Haldar SM, Stamler JS. S-nitrosylation: integrator of cardiovascular performance and oxygen delivery. J Clin Invest. 2013; 123:101–110. [PubMed: 23281416]

Hao G, Derakhshan B, Shi L, Campagne F, Gross SS. SNOSID, a proteomic method for identification of cysteine S-nitrosylation sites in complex protein mixtures. Proc Natl Acad Sci U S A. 2006; 103:1012–1017. [PubMed: 16418269]

Hara MR, Agrawal N, Kim SF, Cascio MB, Fujimuro M, Ozeki Y, Takahashi M, Cheah JH, Tankou SK, Hester LD, et al. S-nitrosylated GAPDH initiates apoptotic cell death by nuclear translocation following Siah1 binding. Nat Cell Biol. 2005; 7:665–674. [PubMed: 15951807]

Hess DT, Matsumoto A, Kim SO, Marshall HE, Stamler JS. Protein S-nitrosylation: purview and parameters. Nat Rev Mol Cell Biol. 2005; 6:150–166. [PubMed: 15688001]

Hessian PA, Edgeworth J, Hogg N. MRP-8 and MRP-14, two abundant Ca(2+)-binding proteins of neutrophils and monocytes. J Leukoc Biol. 1993; 53:197–204. [PubMed: 8445331]

Ho GP, Selvakumar B, Mukai J, Hester LD, Wang Y, Gogos JA, Snyder SH. S-nitrosylation and S-palmitoylation reciprocally regulate synaptic targeting of PSD-95. Neuron. 2011; 71:131–141. [PubMed: 21745643]

Hobbs JA, May R, Tanousis K, McNeill E, Mathies M, Gebhardt C, Henderson R, Robinson MJ, Hogg N. Myeloid cell function in MRP-14 (S100A9) null mice. Mol Cell Biol. 2003; 23:2564–2576. [PubMed: 12640137]

Huang da W, Sherman BT, Lempicki RA. Systematic and integrative analysis of large gene lists using DAVID bioinformatics resources. Nat Protoc. 2009; 4:44–57. [PubMed: 19131956]

Huber R, Berendes R, Burger A, Schneider M, Karshikov A, Luecke H, Romisch J, Paques E. Crystal and molecular structure of human annexin V after refinement. Implications for structure, membrane binding and ion channel formation of the annexin family of proteins. J Mol Biol. 1992; 223:683–704. [PubMed: 1311770]

Ionita MG, Vink A, Dijke IE, Laman JD, Peeters W, van der Kraak PH, Moll FL, de Vries JP, Pasterkamp G, de Kleijn DP. High levels of myeloid-related protein 14 in human atherosclerotic plaques correlate with the characteristics of rupture-prone lesions. Arterioscler Thromb Vasc Biol. 2009; 29:1220–1227. [PubMed: 19520974]

Ismail SA, Park HW. Structural analysis of human liver glyceraldehyde-3-phosphate dehydrogenase. Acta Crystallogr D Biol Crystallogr. 2005; 61:1508–1513. [PubMed: 16239728]

Jia J, Arif A, Ray PS, Fox PL. WHEP domains direct noncanonical function of glutamyl-Prolyl tRNA synthetase in translational control of gene expression. Mol Cell. 2008; 29:679–690. [PubMed: 18374644]

Jia J, Arif A, Willard B, Smith JD, Stuehr DJ, Hazen SL, Fox PL. Protection of extrariboosmal RPL13a by GAPDH and dysregulation by S-nitrosylation. Mol Cell. 2012; 47:656–663. [PubMed: 22771119]

Kim SF, Huri DA, Snyder SH. Inducible nitric oxide synthase binds, S-nitrosylates, and activates cyclooxygenase-2. Science. 2005; 310:1966–1970. [PubMed: 16373578]

Kornberg MD, Sen N, Hara MR, Juluri KR, Nguyen JV, Snowman AM, Law L, Hester LD, Snyder SH. GAPDH mediates nitrosylation of nuclear proteins. Nat Cell Biol. 2010; 12:1094–1100. [PubMed: 20972425]

Laguette N, Sobhian B, Casartelli N, Ringeard M, Chable-Bessia C, Segeral E, Yatim A, Emiliani S, Schwartz O, Benkirane M. SAMHD1 is the dendritic- and myeloid-cell-specific HIV-1 restriction factor counteracted by Vpx. Nature. 2011; 474:654–657. [PubMed: 21613998]

Lee S, Lee HC, Kwon YW, Lee SE, Cho Y, Kim J, Kim JY, Lee J, Yang HM, Mook-Jung I, et al. Adenylyl cyclase-associated protein 1 is a receptor for human resistin and mediates inflammatory actions of human monocytes. Cell Metab. 2014; 19:484–497. [PubMed: 24606903]

Lee TY, Chen YJ, Lu CT, Ching WC, Teng YC, Huang HD, Chen YJ. dbSNO: a database of cysteine S-nitrosylation. Bioinformatics. 2012; 28:2293–2295. [PubMed: 22782549]

Li W, Bengtson MH, Ulbrich A, Matsuda A, Reddy VA, Orth A, Chanda SK, Batalov S, Joazeiro CA. Genome-wide and functional annotation of human E3 ubiquitin ligases identifies MULAN, a mitochondrial E3 that regulates the organelle's dynamics and signaling. PLoS One. 2008; 3:e1487. [PubMed: 18213395]

Lim KH, Ancrile BB, Kashatus DF, Counter CM. Tumour maintenance is mediated by eNOS. Nature. 2008a; 452:646–649. [PubMed: 18344980]

Lim SY, Raftery M, Cai H, Hsu K, Yan WX, Hseih HL, Watts RN, Richardson D, Thomas S, Perry M, et al. S-nitrosylated S100A8: novel anti-inflammatory properties. J Immunol. 2008b; 181:5627–5636. [PubMed: 18832721]

Lipton SA, Choi YB, Takahashi H, Zhang D, Li W, Godzik A, Bankston LA. Cysteine regulation of protein function--as exemplified by NMDA-receptor modulation. Trends Neurosci. 2002; 25:474–480. [PubMed: 12183209]

Ma LP, Haugen E, Ikemoto M, Fujita M, Terasaki F, Fu M. S100A8/A9 complex as a new biomarker in prediction of mortality in elderly patients with severe heart failure. Int J Cardiol. 2012; 155:26–32. [PubMed: 21334078]

Marino SM, Gladyshev VN. Structural analysis of cysteine S-nitrosylation: a modified acid-based motif and the emerging role of trans-nitrosylation. J Mol Biol. 2010; 395:844–859. [PubMed: 19854201]

Marozkina NV, Gaston B. S-Nitrosylation signaling regulates cellular protein interactions. Biochim Biophys Acta. 2012; 1820:722–729. [PubMed: 21745537]

McCormick MM, Rahimi F, Bobryshev YV, Gaus K, Zreiqat H, Cai H, Lord RS, Geczy CL. S100A8 and S100A9 in human arterial wall. Implications for atherogenesis. J Biol Chem. 2005; 280:41521–41529. [PubMed: 16216873]

Nagareddy PR, Murphy AJ, Stirzaker RA, Hu Y, Yu S, Miller RG, Ramkhelawon B, Distel E, Westerterp M, Huang LS, et al. Hyperglycemia promotes myelopoiesis and impairs the resolution of atherosclerosis. Cell Metab. 2013; 17:695–708. [PubMed: 23663738]

Nakamura T, Lipton SA. Emerging role of protein-protein transnitrosylation in cell signaling pathways. Antioxid Redox Signal. 2013; 18:239–249. [PubMed: 22657837]

Nakamura T, Tu S, Akhtar MW, Sunico CR, Okamoto S, Lipton SA. Aberrant protein s-nitrosylation in neurodegenerative diseases. Neuron. 2013; 78:596–614. [PubMed: 23719160]

Nathan C, Calingasan N, Nezezon J, Ding A, Lucia MS, La Perle K, Fuortes M, Lin M, Ehrt S, Kwon NS, et al. Protection from Alzheimer's-like disease in the mouse by genetic ablation of inducible nitric oxide synthase. J Exp Med. 2005; 202:1163–1169. [PubMed: 16260491]

Nicolet S, Herrmann H, Aebi U, Strelkov SV. Atomic structure of vimentin coil 2. J Struct Biol. 2010; 170:369–376. [PubMed: 20176112]

Padgett CM, Whorton AR. S-nitrosoglutathione reversibly inhibits GAPDH by S-nitrosylation. Am J Physiol. 1995; 269:C739–749. [PubMed: 7573405]

Paige JS, Xu G, Stancevic B, Jaffrey SR. Nitrosothiol reactivity profiling identifies S-nitrosylated proteins with unexpected stability. Chem Biol. 2008; 15:1307–1316. [PubMed: 19101475]

Rahaman SO, Zhou G, Silverstein RL. Vav protein guanine nucleotide exchange factor regulates CD36 protein-mediated macrophage foam cell formation via calcium and dynamin-dependent processes. J Biol Chem. 2011; 286:36011–36019. [PubMed: 21865158]

Ray PS, Jia J, Yao P, Majumder M, Hatzoglou M, Fox PL. A stress-responsive RNA switch regulates VEGFA expression. Nature. 2009; 457:915–919. [PubMed: 19098893]

Riva M, He Z, Kallberg E, Ivars F, Leanderson T. Human S100A9 protein is stabilized by inflammatory stimuli via the formation of proteolytically-resistant homodimers. PLoS One. 2013; 8:e61832. [PubMed: 23626736]

Roth J, Vogl T, Sorg C, Sunderkotter C. Phagocyte-specific S100 proteins: a novel group of proinflammatory molecules. Trends Immunol. 2003; 24:155–158. [PubMed: 12697438]

Sampath P, Mazumder B, Seshadri V, Gerber CA, Chavatte L, Kinter M, Ting SM, Dignam JD, Kim S, Driscoll DM, et al. Noncanonical function of glutamyl-prolyl-tRNA synthetase: gene-specific silencing of translation. Cell. 2004; 119:195–208. [PubMed: 15479637]

Schonthaler HB, Guinea-Viniegra J, Wculek SK, Ruppen I, Ximenez-Embun P, Guio-Carrion A, Navarro R, Hogg N, Ashman K, Wagner EF. S100A8-S100A9 protein complex mediates psoriasis by regulating the expression of complement factor C3. Immunity. 2013; 39:1171–1181. [PubMed: 24332034]

Seth D, Hausladen A, Wang YJ, Stamler JS. Endogenous protein S-Nitrosylation in E. coli: regulation by OxyR. Science. 2012; 336:470–473. [PubMed: 22539721]

Seth D, Stamler JS. The SNO-proteome: causation and classifications. Curr Opin Chem Biol. 2011; 15:129–136. [PubMed: 21087893]

Smith BC, Marletta MA. Mechanisms of S-nitrosothiol formation and selectivity in nitric oxide signaling. Curr Opin Chem Biol. 2012; 16:498–506. [PubMed: 23127359]

Smith WJ, Nassar N, Bretscher A, Cerione RA, Karplus PA. Structure of the active N-terminal domain of Ezrin. Conformational and mobility changes identify keystone interactions. J Biol Chem. 2003; 278:4949–4956. [PubMed: 12429733]

van Tits LJ, Hak-Lemmers HL, Demacker PN, Stalenhoef AF, Willems PH. Oxidized low-density lipoprotein induces calcium influx in polymorphonuclear leukocytes. Free Radic Biol Med. 2000; 29:747–755. [PubMed: 11053776]

Vogl T, Ludwig S, Goebeler M, Strey A, Thorey IS, Reichelt R, Foell D, Gerke V, Manitz MP, Nacken W, et al. MRP8 and MRP14 control microtubule reorganization during transendothelial migration of phagocytes. Blood. 2004; 104:4260–4268. [PubMed: 15331440]

Vyas K, Chaudhuri S, Leaman DW, Komar AA, Musiyenko A, Barik S, Mazumder B. Genome-wide polysome profiling reveals an inflammation-responsive posttranscriptional operon in gamma interferon-activated monocytes. Mol Cell Biol. 2009; 29:458–470. [PubMed: 19001086]

Wu C, Parrott AM, Liu T, Jain MR, Yang Y, Sadoshima J, Li H. Distinction of thioredoxin transnitrosylation and denitrosylation target proteins by the ICAT quantitative approach. J Proteomics. 2011; 74:2498–2509. [PubMed: 21704743]

Yun BW, Feechan A, Yin M, Saidi NB, Le Bihan T, Yu M, Moore JW, Kang JG, Kwon E, Spoel SH, et al. S-nitrosylation of NADPH oxidase regulates cell death in plant immunity. Nature. 2011; 478:264–268. [PubMed: 21964330]

Zahid S, Khan R, Oellerich M, Ahmed N, Asif AR. Differential S-nitrosylation of proteins in Alzheimer's disease. Neuroscience. 2014; 256:126–136. [PubMed: 24157928]

Zareba-Koziol M, Szwajda A, Dadlez M, Wyslouch-Cieszynska A, Lalowski M. Global analysis of S-nitrosylation sites in the wild type and APP transgenic mouse brain- clues for synaptic pathology. Mol Cell Proteomics. 201410.1074/mcp.M113.036079
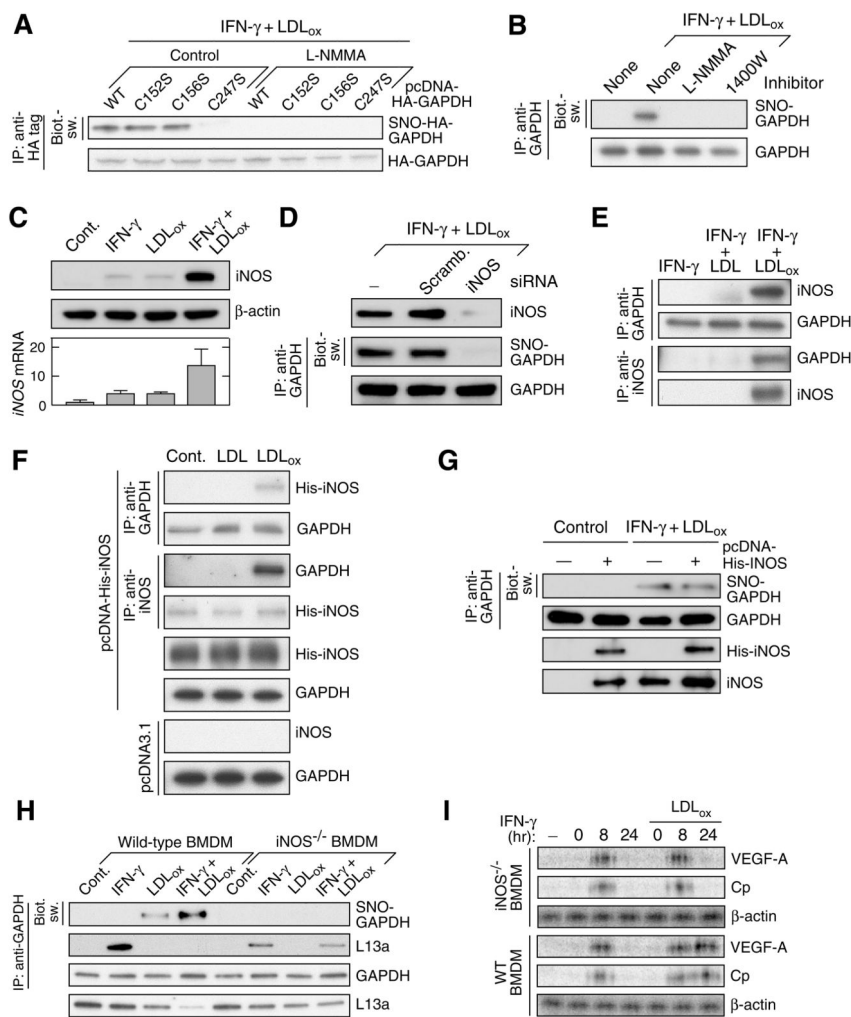
Figure 1. iNOS is Essential for Cys^{247} *S*-Nitrosylation

(A) L-NMMA suppresses GAPDH Cys^{247} S-nitrosylation. Human PBM were transfected with HA-GAPDH (WT and Cys-to-Ser mutant). Cells were pre-incubated for 1 hr with L-NMMA (500 μM) and then treated for 24 hr with IFN-γ (500 U/ml) plus LDL$_{ox}$ (25 μg/ml). Lysates were subjected to immunoprecipitation (IP) and immunoblot (IB) with antibodies indicated. *S*-nitrosylation was determined by biotin-switch (Biot.-sw).

(B) NOS inhibitors block GAPDH S-nitrosylation. PBM were pre-incubated with L-NMMA or 1400W (100 μM), and then with LDL$_{ox}$/IFN-γ. Lysates were subjected to IP and IB or Biot.-sw. analysis.

(C) IFN-γ plus LDL$_{ox}$ induce iNOS expression in human PBM. Protein and mRNA were determined by IB and qRT-PCR respectively. iNOS expression was normalized to β-actin (mean ± SEM, n = 3 experiments).

(D) iNOS is required for inducible GAPDH *S*-nitrosylation. iNOS was depleted by siRNA treatment. Lysates from agonist-treated iNOS-null and control cells were subjected to IB and IP or Biot.-sw. analysis.

(E) LDL$_{ox}$/IFN-γ induces iNOS-GAPDH interaction. PBM were incubated for 24 hr with different agonist. Lysates were subjected to IP and IB with indicated antibodies.

(F) LDL$_{OX}$ induces iNOS-GAPDH interaction. U937 cells were transfected with His-iNOS or empty vector, and then treated with 25 μg/ml native LDL or LDL$_{OX}$. Lysates were subjected to IP and IB with indicated antibodies.

(G) iNOS expression is not sufficient for GAPDH *S*-nitrosylation. U937 cells were transfected with His-iNOS. Lysates from control and treated cells were subjected to IP and IB with indicated antibodies or Biot.-sw. analysis.

(H) Inducible GAPDH *S*-nitrosylation and L13a degradation are iNOS-dependent. BMDM from wild-type or iNOS$^{-/-}$ mice were treated with IFN-γ, LDL$_{OX}$, or both. Lysates were subjected to IP and IB with indicated antibodies or Biot.-sw. analysis.

(I) iNOS contributes to GAIT pathway dysregulation. BMDM from iNOS$^{-/-}$ (top 3 panels) or WT mice (bottom 3 panels) were stimulated for up to 24 hr and then subjected to ^{35}S-Met/Cys metabolic labeling. Lysates were subjected to IP with anti-VEGF-A, -Cp, or -β-actin antibodies, and labeling determined by electrophoresis and autoradiography.
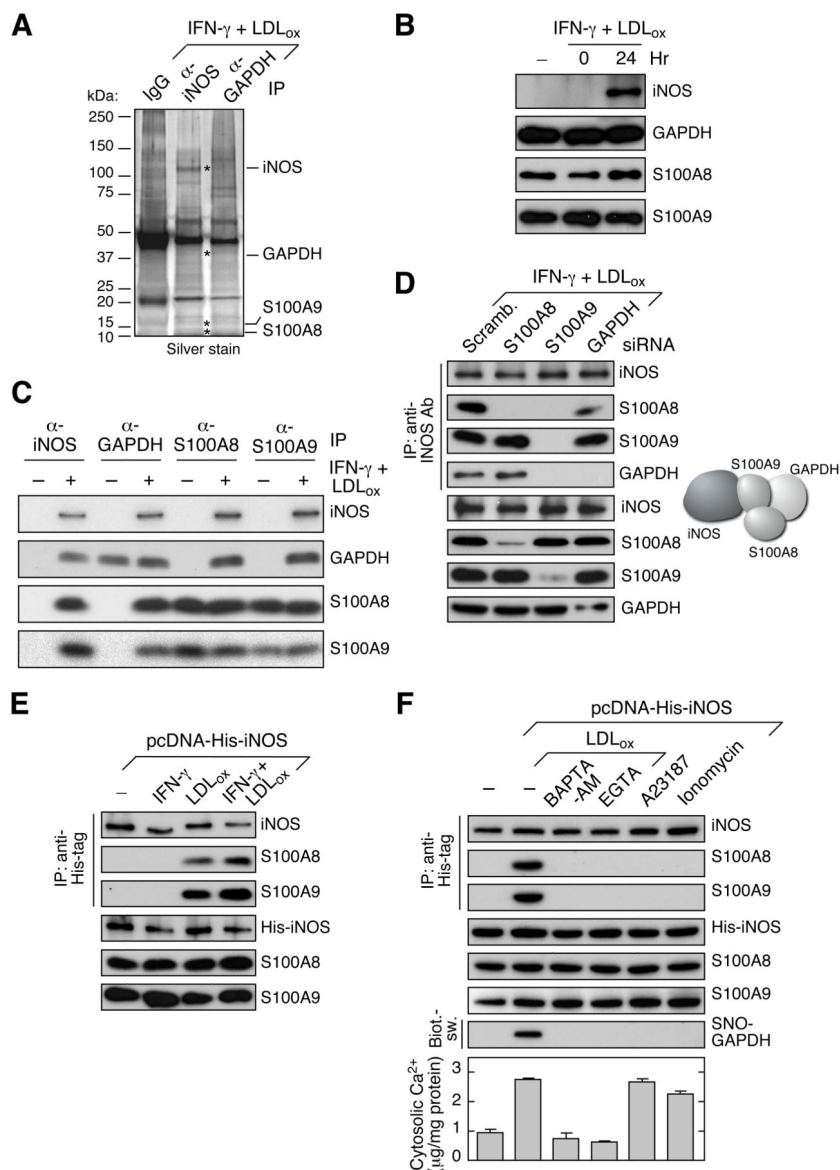
Figure 2. S100A8/A9 Directs iNOS-GAPDH Interaction and GAPDH *S*-Nitrosylation

(A) S100A8 and S100A9 identified as binding partners of iNOS and GAPDH. PBM were incubated for 24 hr with LDL_{ox}/IFN-γ. Lysates were subjected to IP with anti-iNOS or anti-GAPDH antibodies, or control IgG, and analyzed by electrophoresis and silver stain. Specific bands were identified by LC-MS analysis.

(B) LDL_{ox}/IFN-γ does not induce S100A8 or S100A9 expression. Lysates from treated PBM were subjected to IB analysis with antibodies indicated.

(C) LDL_{ox}/IFN-γ induces assembly of iNOS-S100A8/A9-GAPDH complex. Lysates from treated PBM were subjected to IP and IB analysis with antibodies indicated.

(D) S100A9 facilitates binding of S100A8 and GAPDH to iNOS. PBM were transfected with siRNA targeting S100A8, S100A9, or GAPDH. After LDL_{ox}/IFN-γ treatment, lysates from treated cells were IP with anti-iNOS antibody and subjected to IB with antibodies indicated (left). Protein interaction model is shown (right).

(E) LDL_{ox} induces binding of S100A8 and S100A9 to iNOS. PBM were transfected with His-iNOS. After recovery, cells were treated with IFN-γ, LDL_{ox}, or both; lysates from treated PBM were subjected to IP and IB analysis with antibodies indicated.

(F) LDL_{ox}-stimulated intracellular Ca^{2+} is required for iNOS-S100A8/A9 complex assembly and activity. PBM that ectopically expressed His-iNOS were treated with LDL_{ox} in the presence of calcium chelators 15 μM BAPTA-AM or 2 mM EGTA, or with calcium ionophores 5 μM A23187 or 1 μM ionomycin. Lysates were subject to IP and IB with indicated antibodies or Biot.-sw. analysis. Cytosolic calcium was determined with *o*-cresolphthalein at 575 nm, and normalized to total cytosolic protein (mean ± SEM, n = 5 experiments).
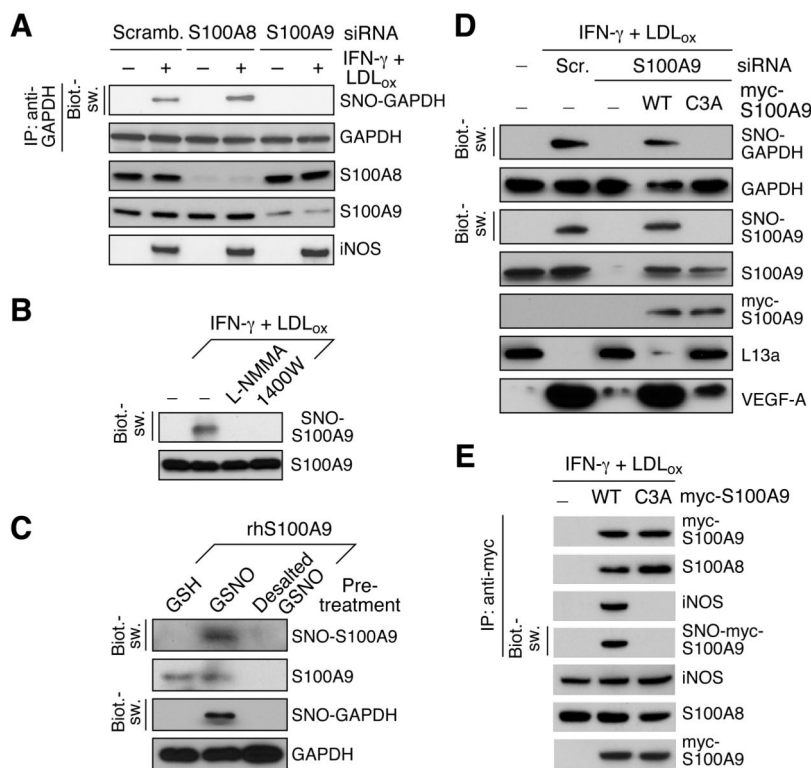
See also Figure S1.

Figure 3. Transnitrosylase Activity of S100A9 Directs iNOS-S100A8/A9 Complex Assembly and GAPDH *S*-Nitrosylation

(A) S100A9 is essential for inducible GAPDH S-nitrosylation. PBM were transfected with siRNA against S100A8 or S100A9 (or scrambled), and then treated with LDL_{ox}/IFN-γ for 24 hr. Lysates were subjected to IP and IB as indicated. GAPDH *S*-nitrosylation was determined by Biot.-sw.

(B) LDL_{ox}/IFN-γ induces *S*-nitrosylation of S100A9. PBM were pre-incubated with L-NMMA or 1400W, and then with LDL_{ox}/IFN-γ. S100A9 *S*-nitrosylation was determined by Biot.-sw. assay.

(C) SNO-S100A9 *S*-nitrosylates GAPDH *in vitro*. Recombinant GAPDH protein was incubated with His-S100A9 pretreated *in vitro* with 100μM GSH or GSNO, or GSNO-desalted buffer as control. *S*-nitrosylation was determined by Biot.-sw. assay.

(D) GAPDH *S*-nitrosylation requires Cys^3 of S100A9. PBM were co-transfected with S100A9 3′-UTR-targeting siRNA and recombinant WT myc-S100A9 or C3A mutant. Lysates from treated PBM were subjected to IB with indicated antibodies or Biot.-sw. analysis.

(E) S100A9 Cys^3 is critical for iNOS-S100A9 interaction. PBM were transfected with recombinant myc-S100A9 (WT or C3A), and then treated with LDL_{ox}/IFN-γ. Lysates from treated cells were subjected to IP and IB with indicated antibodies or Biot.-sw. analysis.
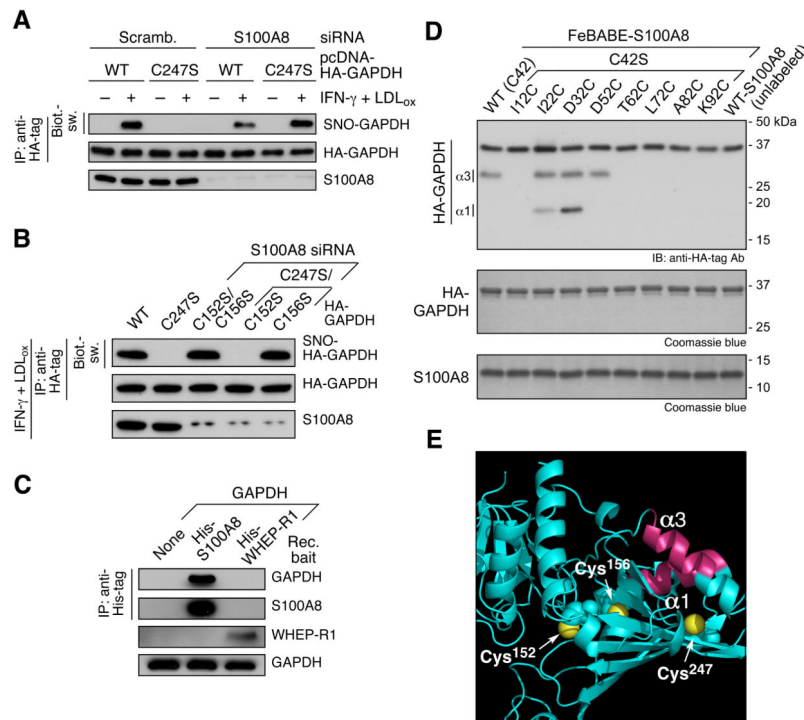
Figure 4. S100A8 Determines Site-Selectivity of the iNOS-S100A8/A9 *S*-Nitrosyl- ase Complex

(A) S100A8 directs selective *S*-nitrosylation of GAPDH. PBM were co-transfected with S100A8-specific siRNA and HA-GAPDH (WT or C247S), and then treated with LDL_{ox}/ IFN-γ for 24 hr. Cell lysates were subjected to IP and IB as shown. Protein *S*-nitrosylation was determined by Biot.-sw.

(B) S100A8 depletion leads to inducible GAPDH *S*-nitrosylation on Cys^{152} and Cys^{247}. PBM were transfected with HA-GAPDH (WT or C247S), or co-transfected with both S100A8 siRNA and HA-GAPDH Cys-to-Ser mutants as indicated. Cells were then treated with LDL_{ox}/IFN-γ. Lysates were subjected to IP and IB or Biot.-sw.

(C) S100A8 by itself binds GAPDH. Purified His-S100A8 and His-EPRS WHEP-R1 protein (as control) were incubated with GAPDH separately. Protein interaction was determined by IP with anti-His-tag antibody and IB with antibodies as indicated.

(D) Fe-BABE determination of S100A8 binding sites on GAPDH. FeBABE-labeled S100A8 bearing cysteine mutations at 10-amino acid intervals in the context of a C42S mutation was incubated with purified N-terminus, HA-GAPDH. Cleavage fragments were determined by IB with anti-HA-tag antibody. Purified recombinant GAPDH and S100A8 proteins were determined by SDS-PAGE and Coomassie blue stain.

(E) Structural model of S100A8 binding domain of GAPDH. GAPDH α-helices α1 and α3 (carmine), and Cys^{247}, Cys^{156}, and Cys^{152} (yellow spheres) are indicated.
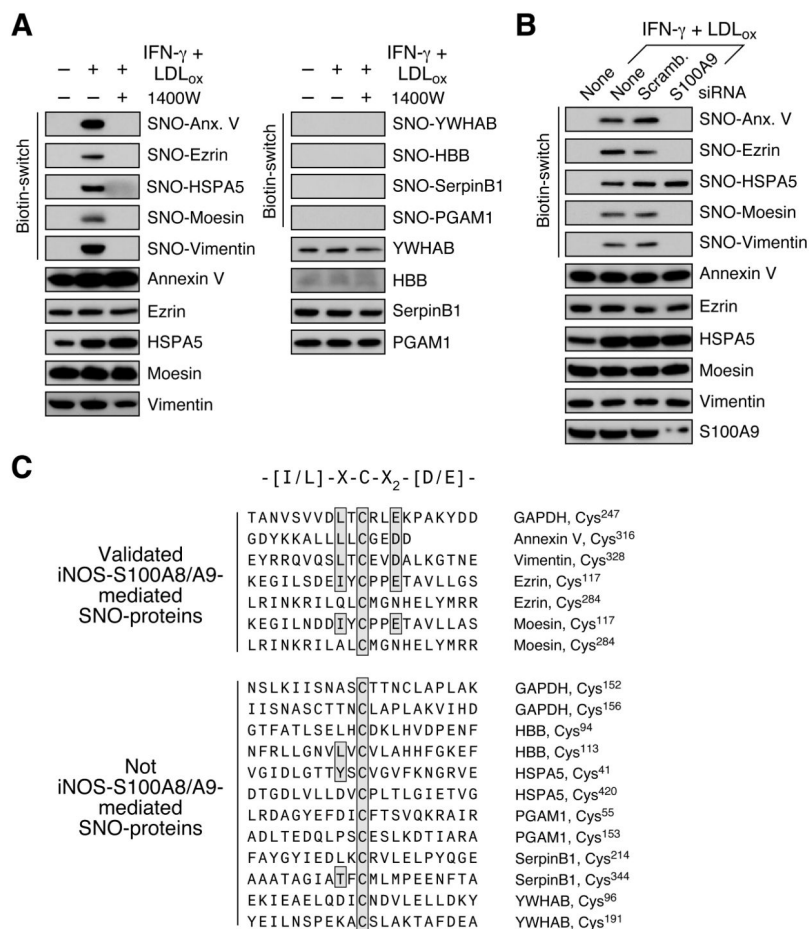
See also Figure S2.

Figure 5. Global *S*-Nitrosylation by the iNOS-S100A8/A9 Complex

(A) iNOS-dependent *S*-nitrosylation of candidates. PBM were pre-incubated with 1400W, and then with LDL$_{ox}$/IFN-γ. *S*-nitrosylated (left) and non-*S*-nitrosylated (right) candidates were determined by Biot.-sw. assay and by IB with antibodies as indicated.

(B) S100A9-dependent *S*-nitrosylation of candidates. PBM were transfected with S100A9 (or scrambled) siRNA, and then treated with LDL$_{ox}$/IFN-γ. *S*-nitrosylation of iNOS-dependent candidates was determined by Biot.-sw. Protein expression was determined IB with antibodies indicated.

(C) Identification of a putative *S*-nitrosylation consensus sequence in iNOS-S100A8/A9-*S*-nitrosylated proteins. Sequences 10 amino acids upstream and downstream from every cysteine in 5 validated SNO-proteins and 12 sites in 6 proteins found to be not *S*-nitrosylated were aligned by Clustal X. Residues conforming to the consensus motif are boxed.
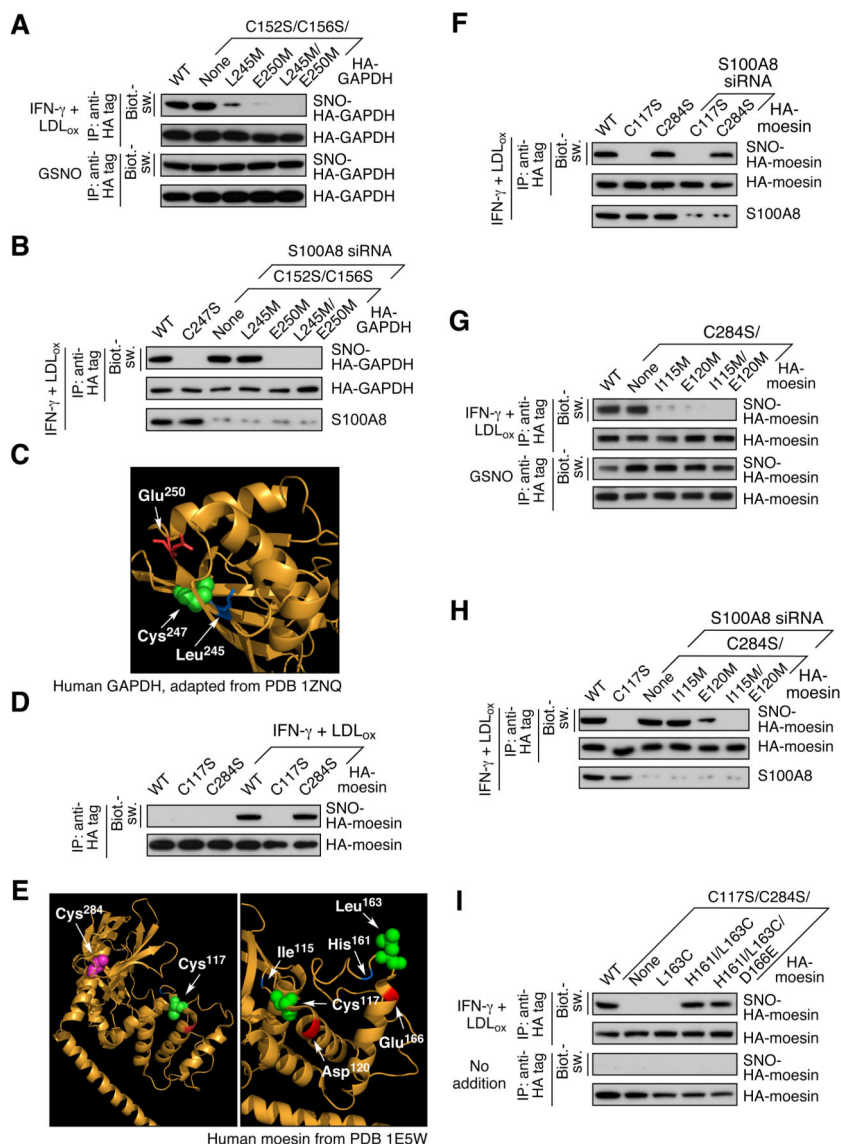
Figure 6. [I/L]-X-C-X$_2$-[D/E] Motif is Necessary and Sufficient for iNOS-S100A8/A9- Directed Protein *S*-Nitrosylation

(A) GAPDH Leu^{245} and Glu^{250} are critical for *S*-nitrosylation of Cys^{247}. PBM were transfected with HA-GAPDH (WT and mutant). Cells were then incubated with LDL$_{ox}$/IFN-γ (top 2 panels) or 1 mM GSNO (lower 2 panels). Cell lysates were subjected to IP and IB as indicated; protein *S*-nitrosylation was determined by Biot.-sw.

(B) S100A8 directs motif recognition in GAPDH *S*-nitrosylation. PBM were transfected with HA-GAPDH (WT or C247S), or co-transfected with S100A8 siRNA and HA-GAPDH mutant. Cell lysates were subjected to IP and IB with antibodies indicated. Protein *S*-nitrosylation was determined by Biot.-sw.

(C) Structural model of *S*-nitrosylation motif in human GAPDH. Leu^{245} (blue), Cys^{247} (green), and Glu^{250} (red) are highlighted.

(D) Identification of *S*-nitrosylation site in moesin. PBM were transfected with HA-moesin (WT or Cys-to-Ser mutant). After recovery, cells were treated with LDL_{ox}/IFN-γ for 24 hr and *S*-nitrosylation of HA-moesin determined by Biot.-sw. assay.

(E) Structural model of human moesin highlighting both cysteine residues and *S*-nitrosylation motif. *Left*, Localization of moesin Cys residues. Ile^{115} (blue), Cys^{117} (green), Glu^{120} (red) and Cys^{284} (purple) are highlighted. *Right,* Model of endogenous and synthetic *S*-nitrosylation motifs in moesin. Ile^{115} (blue), Cys^{117} (green) and Glu^{120} (red) in the conserved motif are highlighted, as are residues mutated in the gain-of-function study, His^{161} (blue), Leu^{163} (green) and Asp^{166} (red).

(F) Absence of S100A8 does not alter moesin *S*-nitrosylation site. PBM were transfected with HA-moesin (WT or mutant), or co-transfected with both S100A8 siRNA and mutated HA-moesin. After recovery, cells were treated with LDL_{ox}/IFN-γ for 24 hr. Lysates from treated cells were subjected to IP and IB with antibodies indicated; *S*-nitrosylation was determined by Biot.-sw.

(G) Ile^{115} and Glu^{120} are critical for Cys^{117} S-nitrosylation of moesin. PBM were transfected with HA-moesin (WT or mutant). After recovery, cells were treated with LDL_{ox}/IFN-γ (top 2 panels) or GSNO (lower 2 panels), and *S*-nitrosylation of HA-moesin determined by Biot.-sw.

(H) S100A8 recognizes *S*-nitrosylation motif of moesin. PBM were transfected with HA-moesin (WT or C117S), or co-transfected with both S100A8 siRNA and HA-moesin mutant. Lysates from treated cells were subjected to IP and IB as indicated; *S*-nitrosylation was determined by Biot.-sw.

(I) Gain-of-function analysis of *S*-nitrosylation motif in moesin. PBM were transfected with HA-moesin (WT or mutant), and then treated with LDL_{ox}/IFN-γ. Cell lysates were subjected to IP and IB as indicated. *S*-nitrosylation was determined by Biot.-sw.
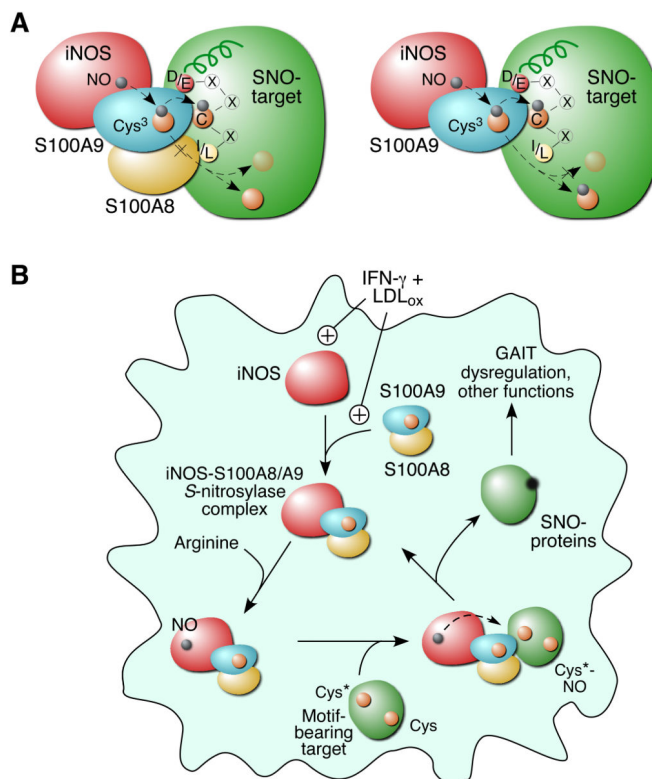
Figure 7. Schematic of iNOS-S100A8/A9-Directed, Site-Selective *S*-Nitrosylation

(A) S100A8 and S100A9 coordinately direct target-selective *S*-nitrosylation by recognition of [I/L]-X-C-X_2-[D/E] motif. NO moiety is transferred from iNOS to S100A9 Cys^3 and then to cysteine in the target motif (left); or to other accessible cysteine residues in the absence of S100A8 (right).

(B) LDL_{ox}/IFN-γ induces iNOS expression, iNOS-S100A8/A9 complex assembly, and target-selective S-nitrosylation, which causes GAIT pathway dysregulation, and is likely to influence other myeloid cell functions.